J ENDOVASC THER
2008;15:643–654

◆ EXPERIMENTAL INVESTIGATION ◆

Effects of Stent Design and Atherosclerotic Plaque Composition on Arterial Wall Biomechanics

Lucas H. Timmins, BS; Clark A. Meyer, BS; Michael R. Moreno, MS; and James E. Moore, Jr., PhD

Department of Biomedical Engineering, Texas A&M University, College Station, Texas, USA.

Purpose: To examine the solid mechanical effects of varying stent design and atherosclerotic plaque stiffness on the biomechanical environment induced in a diseased artery wall model.
Methods: Computational modeling techniques were employed to investigate the final radius of the lumen and artery wall stresses after stent implantation. Two stent designs were studied (one stiff and one less stiff). The stenotic artery was modeled as an axisymmetrical diseased vessel with a 20% stenosis by diameter. The material properties of the diseased tissue in the artery models varied. Atherosclerotic plaques half as stiff (0.5×), of equal stiffness (1.0×), or twice as stiff (2.0×) as the artery wall were investigated.
Results: Final lumen radius was dependent on stent design, and the stiffer stent deformed the artery to an approximately 10% greater radius than the more compliant design. Alternatively, circumferential stress levels were dependent on both stent design and plaque material properties. Overall, the stiffer stent subjected the artery wall to much higher stress values than the more compliant design, with differences in peak values of 0.50, 0.31, and 0.09 MPa for the 2.0×, 1.0×, and 0.5× stiff plaques, respectively.
Conclusion: Evidence suggests that a judicious choice of stent design can minimize stress while maintaining a patent lumen in stenotic arteries. If confronted with a rigid, calcified plaque, stent design is more important, as design differences can impose dramatically different stress fields, while still providing arterial patency. Alternatively, stent design is not as much of an issue when treating a soft, lipid-laden plaque, as stress fields do not vary significantly among stent designs.

J Endovasc Ther 2008;15:643–654

Key words: experimental model, artery wall model, stent, stent design, stress, restenosis, atherosclerotic plaque, finite element analysis

The implantation of a balloon-expandable stent to treat stenotic atherosclerotic disease imposes very high, non-physiologic stresses on the artery wall. The initial acute injury is caused by balloon dilation, which is performed at pressures approaching two orders of magnitude higher than normal physiological pressure. Initial injuries and responses thereto include endothelial denudation, thrombus deposition, and monocyte aggregation.[1] Further chronic injury provokes the processes associated with restenosis (i.e., inflammation, smooth muscle cell/fibroblast proliferation, and matrix protein deposition).

This research was supported by Grant No. R01 EB000115 from the National Institutes of Health (NIH). In accordance with the NIH Public Access Policy, this article is available for open access at PubMed Central.

The authors have no commercial, proprietary, or financial interest in any products or companies described in this article.

Address for correspondence and reprints: James E. Moore, Jr., Department of Biomedical Engineering, Texas A&M University, 337 Zachry Engineering Center, College Station, TX 77843-3120 USA; E-mail: *jmoorejr@tamu.edu*

In cases where the artery is unable to adapt or remodel successfully to this newly imposed biomechanical situation, restenosis results.

Clinical studies have indicated the potential importance of stent design in triggering the restenotic process. Kastrati et al.[2] reported binary restenosis rates varying from 20% to nearly 40% among balloon-expandable stainless steel designs. More recently, in-stent restenosis rates of bare metal versions of modern drug-eluting stents varied from 36.3% for the Bx Velocity stent in the SIRIUS clinical trial to 26.6% for the EXPRESS stent in the TAXUS-IV clinical trial.[3] These clinical studies indicate the importance of stent design, but provide little information that can be used to improve stent design and the biomechanical environment that they impose. In addition, the recent advancements of anti-restenotic strategies, such as drug-eluting stents, aim to counteract the negative effects of the high wall stresses imposed on the artery. However, complications such as late thrombosis[4] and the lack of long-term success in peripheral arteries[5] still limit this technology. A further investigation into the artery wall stresses induced by stent implantation and the pursuit of strategies to minimize them could reduce restenosis rates for both bare metal and drug-eluting stents.

The geometric configuration of the stent struts is a principal determinant of the subsequent chronic stresses in the artery wall. Since stresses cannot be directly measured even in ideal circumstances (they are inferred from separate measurements of force and area), researchers have turned to computational modeling, such as the finite element method (FEM), to estimate the artery wall stresses induced by different designs. In the construction of such models, one must carefully consider the nature of the artery wall model, as modeling is limited by the material models used to characterize arterial and stenotic tissues. Using high-resolution imaging and digital reconstruction techniques, it is possible to model diseased segments of specific patients. Such imaging methods have been utilized to investigate the effects of commercially available stent designs on the mechanical environment within diseased iliac arteries comprised of numerous different vascular tissues, each with unique mechanical properties.[6,7] These studies indicate that specific stent designs can be assessed to determine their mechanical performance on ''virtual'' patients before implantation. While such studies demonstrate the importance of stent design, they are somewhat limited to that particular patient's lesion geometry and its composition. Further advancement in imaging techniques, optical coherence tomography, intravascular ultrasound, and magnetic resonance imaging, have allowed better characterization of the histological components of atherosclerotic plaques and have considerable potential to better assist in the development of patient-specific modeling.[8]

An alternate strategy is to construct more ''generic'' models of the artery wall that are more suitable for delineating differences between stent designs. Generic models of the artery wall (with or without diseased segments), while appearing less relevant to the clinical application, have some advantages in the investigation of the effects of stent design. The applicability of the findings extends beyond a single patient, and one can test stent design variations without having to vary deployment parameters, such as the rotational position of the stent relative to the specific plaque geometry. Lally et al.[9] analyzed the biomechanical interaction between both the S7 and the NIR stent designs in an idealized stenosed coronary artery. Artery and plaque material properties varied and were determined by curve-fitting data from the mechanical testing of human femoral artery and calcified plaque tissue, respectively. The authors concluded that the S7 stent design induced lower stresses on the artery wall compared to the NIR design, which correlates well with observed clinical restenosis rates. Bedoya et al.[10] used a straight, non-diseased model of the artery wall to investigate the effects of varying design parameters of a ring segment stent on artery wall stress and radial support. They found that stents with large axial spacings and ring amplitudes imposed less stress on the artery wall. The final lumen diameter was approximately the same for the different designs.

The inclusion of more realistic geometrical features, such as diseased segments, would

improve the clinical relevance of these studies. However, there are some key issues that arise in this pursuit. First, one must specify the mechanical properties of the plaque, notably a challenge since histological examination has demonstrated the heterogeneity of atherosclerotic plaques. In addition, mechanical testing has shown that the mechanical properties of the various tissue components (fatty streaks, lipid pool, fibrous cap, and calcium deposits) span orders of magnitude.[11] In particular, one investigation that examined the stress-relaxation response of various atherosclerotic plaque specimens (i.e., highly calcified, fibrotic, lipid-laden specimens) reported elastic moduli values ranging from 40 to 3300 kPa.[12] Generally, atherosclerotic plaques are considered to be either less stiff than a typical artery wall, as would be the case in lipid-laden plaques, or much stiffer than the artery wall, as occurs with increased calcification. As Hayashi[13] reported in a review of experimental studies of the material stiffness of diseased arterial tissue, 33% of the studies showed an increase in incremental elastic modulus, 27% showed a decrease, and 40% had no significant change compared to non-diseased tissue. Such variations in tissue material properties are likely to affect the biomechanical environment (wall stresses, radial deformation) induced by the implanted stent. Additional issues include the choice of plaque geometry (i.e., concentric, axisymmetrical). Choosing to vary both plaque material properties and geometry in addition to varying the stent design is not feasible, as the number of simulations required to cover the physiological parameter space quickly becomes overwhelming.

The goal of this study was to determine the effects of varying stent design parameters on the final lumen radius achieved and the stress induced in diseased axisymmetrical artery wall models. Interpretation of the results focused on the effects of varying the mechanical properties of the plaque, since this is most likely to impact the predicted stresses, as well as the final lumen diameter. Thus, we chose to investigate plaques that were less stiff (0.5×), of equal stiffness (1.0×), or stiffer (2.0×) than the artery wall. Hopefully, this study and others in the literature will provide a variety of bases for improving stent design overall and, perhaps more importantly, guidance for lesion-specific stenting.

METHODS

A computational approach was employed to determine the biomechanical impact of varying stent design in stenotic vessels whose atherosclerotic plaques ranged in material stiffness. Two stent models selected from the extreme designs identified in Bedoya et al.[10] were intended to represent designs that have high and low radial rigidity. The multiple step computational simulations began with overexpansion of the stenotic vessel, followed by translation of the stent into the diseased region, and finally reduction of the vessel internal pressure to systolic, followed by diastolic. The mechanics of contact between the two elastic bodies (stent and vessel) was modeled, which determined the final geometrical configuration of the combined structure. The stent geometry was specified in the already expanded state, with uniform mechanical properties and no internal stresses. The artery wall model featured non-linear strain-stiffening properties, and the plaque was specified in separate models as being stiffer, less stiff, or having the same stiffness as the artery wall.

Model Geometry

The 3-dimensional (3D) stent geometries investigated in this study have been previously reported.[10] Briefly, stent models were defined by 3 parameters: strut spacing, radius of curvature, and axial amplitude. The 2 stent designs modeled were those that imposed the highest (stent 1Z1) and lowest (stent 2B3) values of circumferential stress and radial displacement in the aforementioned investigation. Stent 1Z1 was characterized by a strut spacing of 1.2 mm, radius of curvature of 0 mm, and amplitude of 0.6 mm, while stent 2B3 was described by parameter values of 2.4 mm, 0.3 mm, and 1.8 mm, respectively (Fig. 1). Stent designs had a constant strut thickness of 100 μm and a deployed outer radius of 2.475 mm, ~10% larger (1.1 to 1.0 stent-to-artery ratio) than the intimal radius of

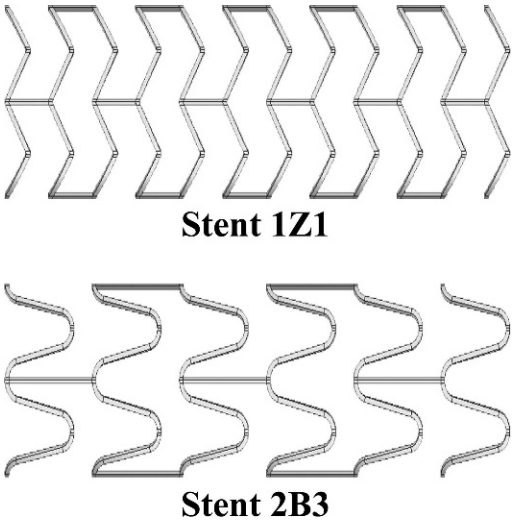

Figure 1 ◆ Illustrations of the stent designs employed in this investigation. The 1Z1 design has a high radial stiffness and induces high radial displacement and stress on the artery wall. The 2B3 design has a lower radial stiffness and places less radial displacement and stress on the artery wall.[10]

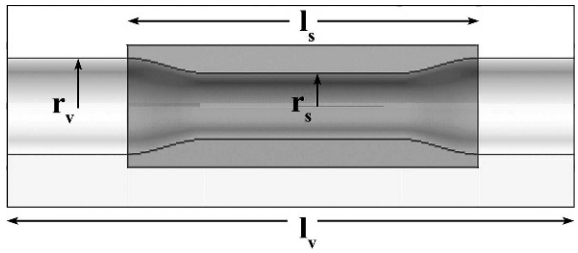

Figure 2 ◆ Undeformed geometry of the diseased models used in this investigation: vessel radius (r_v), stenosis radius (r_s), vessel length (l_v), stenosis length (l_s). The white region denotes healthy arterial tissue and the dark region denotes the atherosclerotic plaque. The stent was ''deployed'' only in the diseased region.

a healthy region (white area in Fig. 2) of the vessel at systole. These geometrical values agree with manufacturers' recommendations and common stenting practice.[14] Due to the repeating nature of ring segments in stent designs and the fact that any edge effects have dissipated within the first ring segment, the biomechanical environment within the middle section of the stent model was equivalent to that of any 2 inner rings of a full length stent. Thus, only a portion (9 mm in length) of a full length was modeled: 8 ring segments for stent 1Z1 and 4 ring segments for stent 2B3. The near-periodic pattern of the resulting stresses near the middle rings supported the validity of this assumption. The material of the stent was modeled as 316L stainless steel [Young's modulus (E) = 200 GPa, Poisson's ratio (v) = 0.3].

The diseased artery was modeled as a generalized stenotic vessel characterized by an 18-mm-long cylinder with a localized concentric atherosclerotic plaque (Fig. 2). The plaque was designed to be a maximum stenosis of ~20% by diameter at diastolic pressure (i.e., equivalent to a residual plaque burden of 20% after stent implantation). The model was representative of a tighter stenosis that had been balloon-expanded and fractured, which agrees with angiographic results from postdilation of clinically significant stenoses.[15] Note that this investigation was focused on the biomechanical environment after the balloon has been deflated and retracted, leaving the stent at its expanded diameter (i.e., focus is placed on the chronic stent-induced stress). Thus, further complexities associated with plastic deformation of the stent and possible plaque fracture during dilation were avoided. Also, the requirement to have the stenoses hold approximately the same shape at physiological axial stretch and diastolic pressure meant that each had a different unloaded geometry (Fig. 3).

The material properties of the artery have been previously utilized in computational models.[10,16] The same form of the strain energy function (SEF) was used to describe the plaque material properties. The plaque stiffness was adjusted by scaling the constants in the SEF (Fig. 4) to represent atherosclerotic plaques 0.5, 1.0, and 2.0 times as stiff as the vessel. The range of mechanical plaque properties investigated fell within the range of experimental data for atherosclerotic tissue[11] and other computational studies of stented diseased vessels.[17]

FEM Simulations

The 3D FEM models were constructed using MSC.Patran 2005 r2, while MSC.Marc

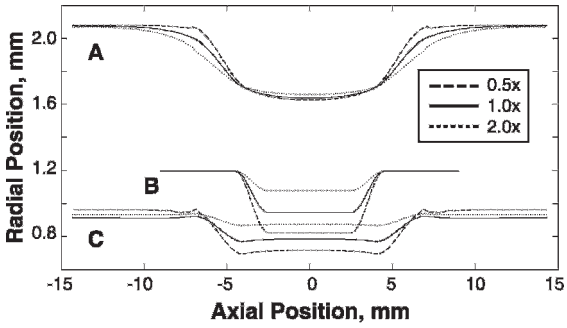

Figure 3 ◆ Unloaded stenosis geometries. Due to the variation in plaque material properties, the unloaded geometries of the stenosed arteries varied (unloaded in **B**, stretched in **C**, stretched and pressurized at 80 mmHg in **A**) to ensure that each model had the same radial dimensions at diastolic pressure (~20% stenosis by diameter). The lines represent plaque stiffness relative to the artery wall: the dashed lines are 0.5×, the solid lines are 1.0×, and the dotted lines are 2.0×.

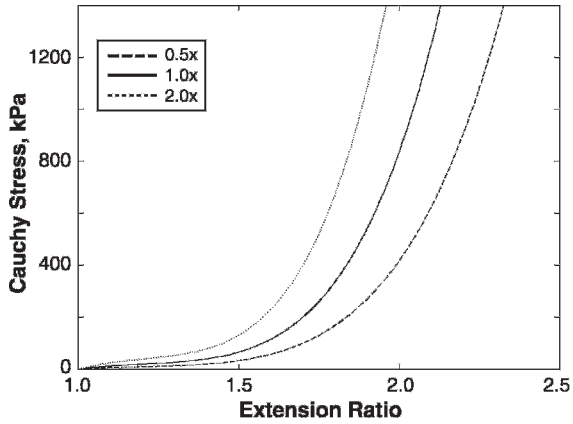

Figure 4 ◆ Material responses used to describe the arterial wall and atherosclerotic plaque. The strain energy function constants were scaled to model plaques that were half as stiff (0.5×, dashed), of equal stiffness (1.0×, solid), or twice as stiff (2.0×, dotted) as the artery wall.

2005 v1 was employed as the non-linear solver (MSC Software, Santa Ana, CA, USA). Displacement, pressure, and contact boundary conditions were applied in multiple stages (fixed load increments). Initially, an axial stretch ratio of 1.59 was applied to the vessel to simulate in vivo longitudinal tethering. A pressure was then applied to the inner surface of the vessel (varied between 660 and 1000 mmHg depending on plaque material properties), inflating the inner radius to a position larger than the outer radius of the oversized stent. Note that these overinflation pressures were not directly related to balloon expansion, but rather were required to ensure proper apposition of the strut to the artery wall. The stent was then translated in the axial direction until the midpoints of the stent and artery overlapped. The inner pressure was then reduced to a systolic value (120 mmHg) and finally diastolic (80 mmHg). Throughout the simulation, constraints were applied to both the artery and stent symmetry edges to restrict rotation and allow only in-plane deformations.

To optimize computational resources, only a quarter of the circumference of the stent and artery were modeled. Furthermore, a non-uniform mesh of the vessel was constructed in which the stented region was twice as dense as the non-stented region. The models were discretized using 20-node hexahedral elements, with total element numbers of 922, 938, and 19,320 for stents 1Z1, 2B3, and the vessel, respectively. Displacements were interpolated using quadratic Lagrange functions, and contacting bodies were defined with a C^2-continuous non-uniform rational B-splines surface. The mesh was considered converged when circumferential wall stress and deformed radial position values at diastolic pressure differed by $<2\%$ and $<1.25\%$, respectively, while doubling the mesh density of the stented region in all principal directions (r, θ, z).

Evaluation Methods

To examine differences among stent designs, as well as the material properties of the plaques, the biomechanical (radial displacement, wall stress) impact of stent deployment in stenotic arteries was analyzed. From a clinical standpoint, radial position was of utmost importance for stenting procedures, as sufficient displacement was required to restore blood flow to downstream tissues. As a measure of each stent design's ability to maintain a patent lumen, the deformed radial position achieved by each design on the

various plaque properties was evaluated. As studies have shown that arteries remodel in response to increased levels of blood pressure (i.e., hypertension)[18] and arterial cellular components respond to varying levels of cyclic stretch,[19] it is thought that changes in the normal physiological mechanical environment result in a biological response that aims to restore mechanical values (wall stress, fluid shear stress) to homeostatic levels. Thus, it has been hypothesized that neointimal growth is a direct result of the extremely high, non-physiological stresses induced by the stent onto the artery wall. Circumferential (hoop) stress values in the artery wall were compared to two representative measures of wall stress. Using analytical techniques described below, values at the original location of the intima were examined, as it was a preferred location to detect biomechanical differences that may be related to restenosis due to its immediate proximity to the internal elastic lamina (IEL). Disruption of the IEL has been shown to greatly increase the risk of restenosis development.[20,21] Average stress values through the thickness were also analyzed; such values can be compared to Law of Laplace values to examine the impact of stent deployment on the averaged stresses induced on the artery wall.

Results from the FEM simulations, which were used for post-processing calculations, were reported as nodal values corresponding to radial displacement and circumferential stress at diastolic pressure. Radial displacement values were used along with undeformed radial locations to determine final lumen position after ''implantation'' of the stent. Deformed radial position values of the intimal surface were averaged around the circumference (θ-averaged) along the length of the deformed artery. Circumferential stress fields from each FEM simulation consisted of average circumferential stress plots at the location of the IEL. Circumferential stress values at the IEL were determined by quadratic interpolation from nearby nodal values (i.e., nodes shared the same undeformed circumferential and axial location). As described above, the interpolated values were averaged around the circumference along the length of the deformed artery.

RESULTS

The final inner radius of the stented artery was found to depend strongly on the stent design, but very weakly on the plaque properties. Deployment of the stiffer stent (1Z1) resulted in a final inner radius of $\sim$2.47 mm in the stented region for all plaque material properties, while deployment of the more compliant stent (2B3) resulted in a final radius of $\sim$2.27 mm (Fig. 5). The inner radius of the unstented artery outside the plaque was 2.07 mm at diastolic pressure, so both stents would have been considered clinically successful (both stents were oversized 10%). There was a slight inward motion near the edges of the stent with the stiffest plaque and for the more compliant stent. This occurred due to the stiff plaque pushing inward at the edges of the stent, the part of the structure with the least radial strength. The final radius in the stiffer stent was nearly uniform along the length of the stent, with sharp drop-offs at the ends. In the more compliant stent, the final radius tapered off more gradually at the ends.

Circumferential stress values at the original arterial intima, representative of the location of the IEL, were higher in the presence of a stiffer plaque and were dependent on stent design. Examination of the peak stress values (θ-average) in the stented region revealed that the largest differences in circumferential stress attributable to stent design were observed with the stiffest plaque. The peak circumferential stress value in the stented region was 1310 kPa with the 2.0$\times$ plaque and the stiffer stent (1Z1) versus 803 kPa with the more compliant stent (2B3) and the same plaque (Fig. 6). With the 1.0$\times$ plaque, the peak circumferential stress was 750 kPa with the stiffer stent (1Z1) and 443 kPa with the more compliant stent (2B3). The smallest differences between stent designs were observed with the 0.5$\times$ plaque. In this case, the peak circumferential stress was 262 kPa with the stiffer stent (1Z1) versus 158 kPa with the more compliant stent (2B3). As with radial displacement, the circumferential stress field was more uniform along the length of the stiffer stent, while it tapered off more gradually at the edges of the more compliant stent.

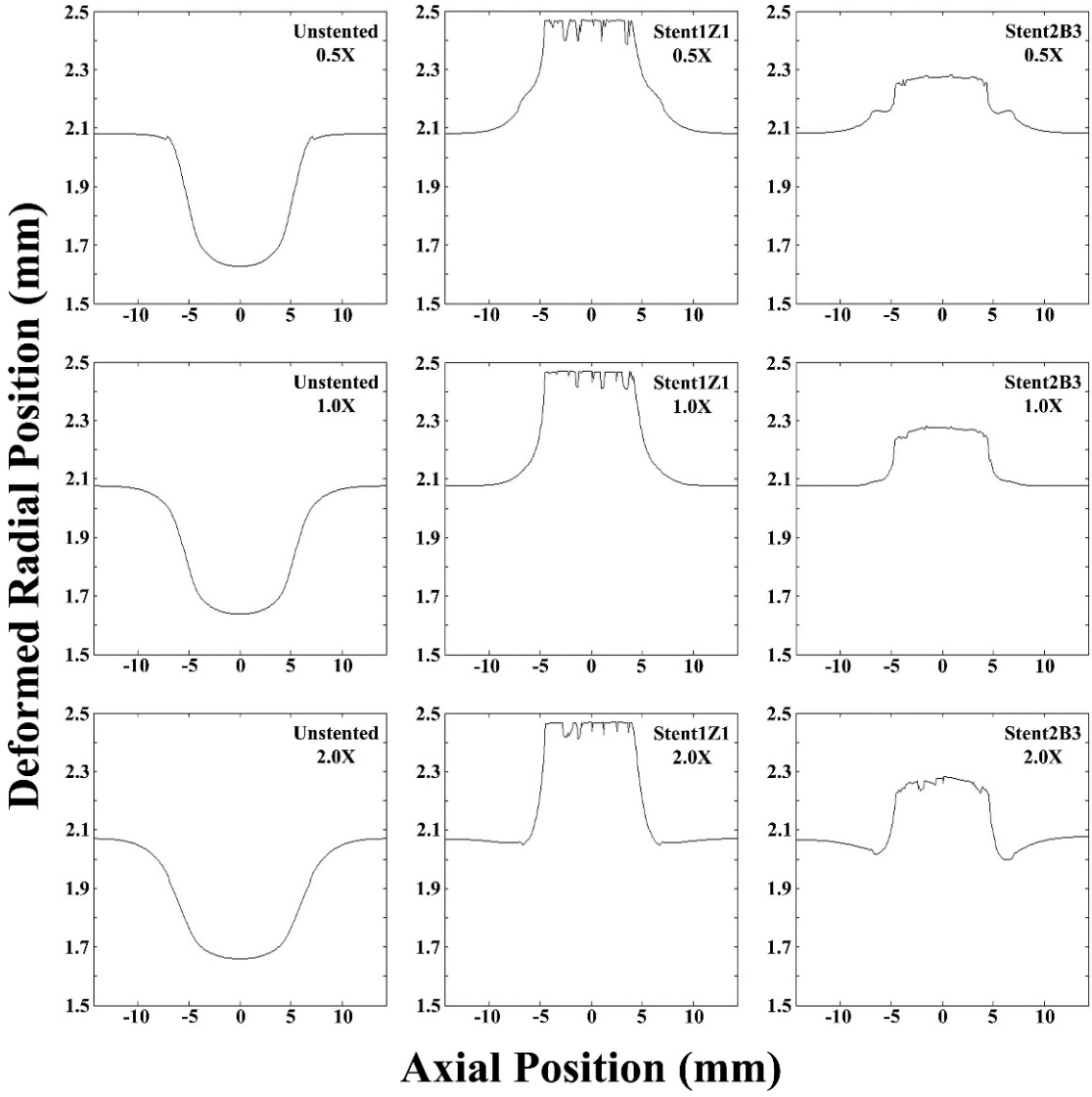

Figure 5 ◆ Final inner radial positions (lumen radius). Deformed radial position values were determined by averaging around the circumference of the vessel at diastolic pressure along the vessel axis. The final radial position was dependent only on stent design and not plaque material properties. The stiffer (1Z1) and more compliant (2B3) stent designs propped open the artery to ~2.47 and 2.27 mm, respectively, despite the change in plaque material properties.

Mean (averaged through the thickness) circumferential artery wall stresses were substantially higher for the more rigid stent (1Z1) design and an order of magnitude higher than that predicted by the Law of Laplace for an unstented artery (both healthy and diseased). As a reference, the Law of Laplace predicted a mean stress value of 35.5 kPa for the healthy region of the vessel, whereas a value of 22.0 kPa was calculated for the stenotic region, both at diastolic pressure. In the presence of the more rigid stent (1Z1), mean stress values in the middle 50% of the stent (i.e., the region where the ring segments would repeat in a full length stent) were 465, 425, and 411 kPa for the 2.0×, 1.0×, and 0.5× plaque stiffnesses, respectively. The more compliant stent (2B3) design induced considerably lower mean stress values of 283, 255, and 257 kPa for the plaque

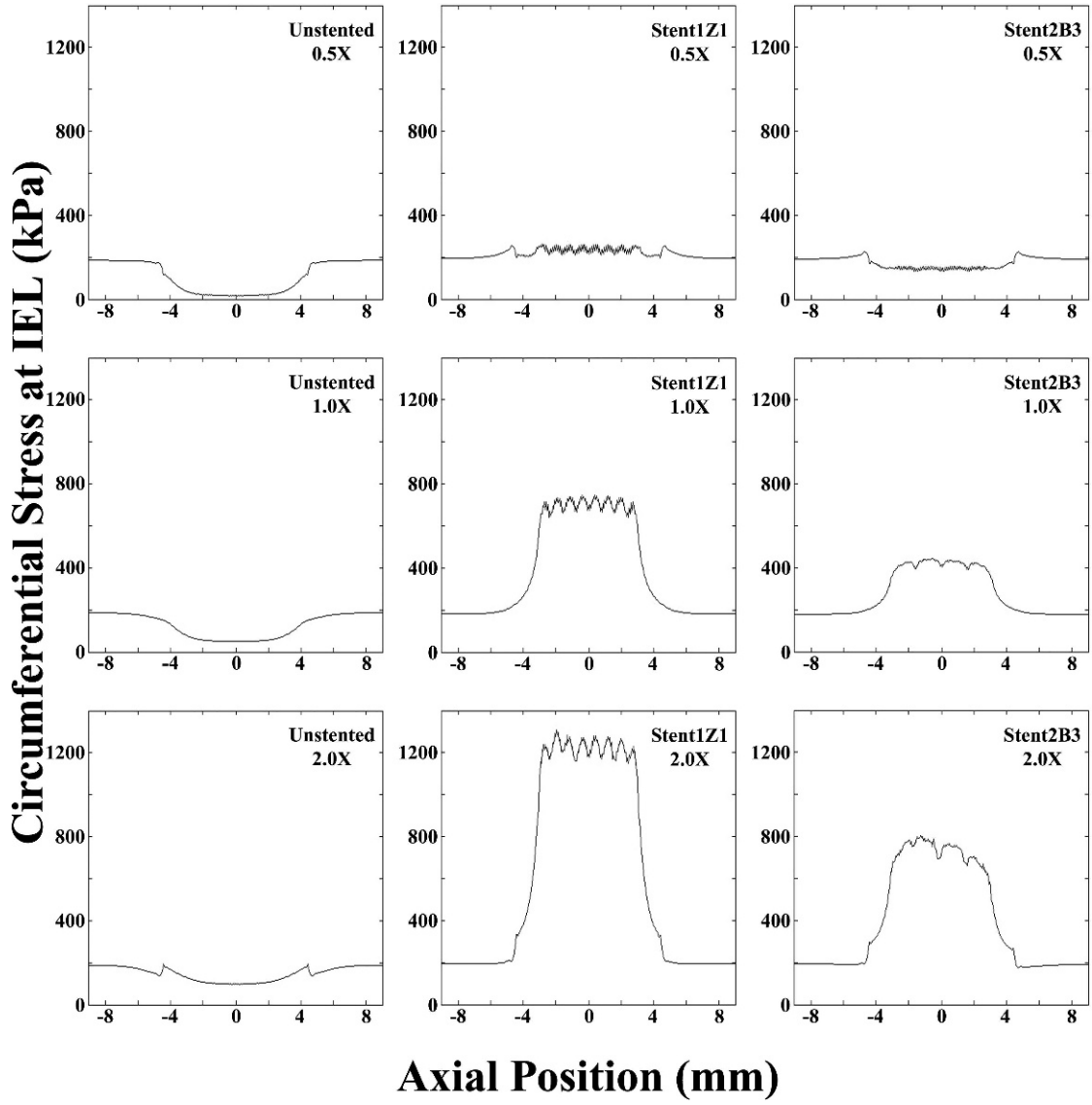

Figure 6 ◆ Artery wall hoop stress values (averaged over the circumference) at the internal elastic lamina (IEL) were dependent on both stent design and plaque material properties. Highest stress values were observed for the stiffest plaque (2.0×) and most rigid stent (1Z1), while the smallest values were seen for the least stiff plaque (0.5×) and more compliant stent design (2B3). Note high circumferential stress values at the IEL are most likely to disrupt this structure, provoking neointimal growth leading to restenosis.[20,21]

stiffnesses of 2.0×, 1.0×, and 0.5×, respectively.

The range of circumferential stress experienced by the IEL around the central portion of the stented plaques was much higher with the stiffer plaques and depended on stent design. The maximum circumferential stress typically occurred adjacent at the point where the struts contacted the plaque, while the minimum circumferential stress occurred at points removed from the strut locations. Within the middle 50% of the stented length, circumferential stress values ranged from 1160 to 1310 kPa, with an average value of 1230 kPa, for the more rigid stent (1Z1) and stiffest 2.0× plaque (Fig. 6). In the case of the more compliant stent (2B3) design in the 2.0× plaque, the stress values ranged from 663 to

803 kPa (mean 746 kPa). Decreasing the plaque stiffness resulted in decreases in both the range of circumferential stresses and the average induced at the location of the IEL. With the 1.0× plaque stiffness, circumferential stress values of 662, 749, and 708 kPa corresponding to the minimum, maximum, and average stress values, respectively, were observed for the 1Z1 stent design. The corresponding values for the 2B3 design in the 1.0× plaque stiffness were 390, 443, and 425 kPa, respectively. For the least stiff plaque (0.5×) models, both the range of circumferential stresses induced and the average were lower and more similar between the stent designs. Stress values of 209, 262, and 237 kPa for the minimum, maximum, and average values, respectively, were found for the rigid (1Z1) design, whereas values of 132, 158, and 147 kPa were observed for the more compliant stent (2B3).

Examination of the stent edges revealed very abrupt changes in circumferential stress over small distances (i.e., high stress gradients). For the case combining the stiffest plaque (2.0×) and stent (1Z1), average circumferential stress values varied rapidly by ~748 kPa over distances of <1.0 mm. For the same plaque stiffness, the more compliant stent (2B3) design had stress changes of ~341 kPa over the same distance. The same trend held for the 1.0× case, where the stiff stent had larger changes (407 kPa) than the more compliant design (154 kPa) over a distance of <1.0 mm. The least stiff plaque (0.5×) saw the smallest difference between designs, with circumferential stress changes of 57.6 and 4.45 kPa for the stiffer (1Z1) and more compliant (2B3) designs, respectively, over <1.0 mm distances.

DISCUSSION

The biomechanical implications of stent implantation include dramatic changes in artery wall stress and flow patterns. While these effects in general are consequences of the clinical need to prop open the artery, there are strategies that designers and clinicians can undertake to minimize the deleterious role biomechanics can play in the restenosis process. Studying the effects of stent design on artery wall stress, followed by an informed choice of the most appropriate stent design for a particular plaque, is one such strategy. We have investigated the effects of stent design on stresses in the walls of arteries with plaques representative of the variety encountered clinically (less stiff, equally stiff, or more stiff than the artery wall). In order to preserve the general applicability of the results, the plaque geometries were rather ''generic'' in nature (i.e., axisymmetrical). The results indicate that stent design and plaque composition combine to determine stress at the location of the IEL and that a judicious choice of stent design can minimize stress at this location while maintaining arterial patency.

In all cases studied here, the stents were successful in establishing a patent lumen, as values of final percent stenosis after the implantation agree with clinical data.[22] The degree to which the artery was propped open was approximately constant for a given stent design, with a negligible degree of dependence on the plaque properties. The stiffer stent resulted in a larger final diameter than the more compliant stent, but the differences were small and not likely to result in a clinically significant difference in acute blood flow restoration. In the case of the stiffest plaque and most compliant stent, there was a slight inward motion of tissue at the edges of the stent, which highlights the importance of insuring that the stent is of sufficient length.

In contrast to the results for deformed radial position, the stress in the artery wall depended on both stent design and plaque properties, with the differences between stents being more pronounced for the stiffer plaques. It should be noted that there is no explicit stress level (value) known to lead to an adverse biological response (inflammation, neointimal hyperplasia, etc.). Stress values at the level of the IEL, at diastolic pressure, were as much as 1310 kPa (1Z1 design, 2.0× plaque stiffness) or ~6.72 times the stress at the IEL in the normal artery wall. Peak stresses at the IEL were much lower for the softest plaque (0.5×), and both peak and average stress values differed only by 104 and 90.1 kPa, respectively. Thus, for a relatively soft, lipid-laden plaque, the more rigid stent design would be preferable to implant, as

there is not a considerable difference in the stress subjected onto the artery compared to the other design and a much larger radial displacement. Alternatively, for a rigid, calcified plaque, the more compliant stent design would be preferred as it would still provide sufficient radial support while greatly reducing chronic injury to the artery wall. In all cases with the stiffer stent, the entire stented region was subjected to a relatively uniform high stress. With the more compliant stent, the stress tapered off at the ends (a sign of ''compliance matching,'' see Berry et al.[23]), and there was a greater degree of heterogeneity around the circumference at a given axial location. While it is certainly likely that the value of the maximum stress is the principal determinant of IEL rupture, chronic average stress values in the stented region could also lead to adverse biological responses. Whether maximum or average stress values are more important in the development of neointimal tissue remains to be elucidated. It is also possible that local gradients in stress trigger cellular proliferation to a degree that influences restenosis.

We have limited the presentation of stress results to the approximate location of the IEL because the disruption of this structure has been linked to a greater risk for restenosis.[20,21] In general, stress varies from very high values at the inner wall to much lower values at the outer wall due to two factors. First, the expansion of an incompressible cylindrical structure results in a higher strain at the inner than at the outer wall, with the difference related to the local wall thickness. Second, the non-linear (strain stiffening) behavior of the artery wall material essentially amplifies the strain difference so that the stresses at the inner wall are higher than those at the outer wall by a greater degree of proportionality than with strain. On the surface of the plaque, where wall thickness is highest, extremely high circumferential stresses (on the order of 2.5 MPa) were predicted in our model, but not reported in the results. Such high stresses are likely to result in plaque fracture, which is indeed a common observation in plaques that have been subjected to balloon angioplasty alone.[24]

Limitations

As with any modeling study, there are several limitations that should be recognized, the most obvious being the assumed symmetry and homogeneity of the plaque and artery. Any effort to model a plaque with a more realistic geometry must address the basic question, ''Which plaque?'' There are, of course, a tremendous number of plaque geometries, just as there are numerous plaque mechanical properties. Therefore, we have chosen to study variations in plaque mechanical properties, sacrificing specificity in geometry in favor of more generality in the applicability of the results. Further studies of the effects of plaque geometry are certainly warranted, but inherently much more computationally demanding than the work presented here in terms of numbers of models required and the need to model a full circumference of stent and artery.

It was assumed that only elastic deformation occurred in all structures (artery, plaque, and stent). Therefore, we have chosen not to include plaque fracture or damage in our models, so the stresses predicted in the plaque itself may not be reliable (i.e., fracture would likely occur at much lower stress values). While there are studies that have investigated atherosclerotic plaque fracture,[25] it is an event that is highly dependent on plaque geometry and composition and thus is highly patient specific.

We have also limited our study of plaque properties to a range between 0.5× and 2.0× the native artery stiffness. When assessed with appropriate finite deformation models, it is likely that a wider range of plaque properties could be identified, yet the stiffness values examined are within the range of available experimental data,[26] as well as other computational studies.[17] The range of stent designs could also be extended. In both cases, it is likely that the general trends exhibited here (higher stress with stiffer plaques, stiffer stents, etc.) would hold.

In addition, the stent expansion process was not modeled, so any material inhomogeneities that could result from plastic deformation are not taken into account (i.e., it was assumed that the homogeneous material

properties of the stents were identical upon initiation of contact with the artery wall), although it is also not likely to change the trends. It should also be noted that vascular stenting causes non-laminar flow patterns to develop within a stented artery, as both computational and experimental studies have shown.[27–29] While only the solid mechanical environment was investigated in this study, both solid and fluid mechanical factors should be considered when optimizing stent design and improving the long-term patency of these devices.

Conclusion

In this study, variations in stent design were investigated to determine their impact on the biomechanical environment in diseased vessels with varying plaque material properties. The position of the lumen after stent deployment was dependent only on stent design, with the stiffer stent (1Z1) propping open the artery to a larger radial value. Also, the displacement field was much more uniform with the stiffer stent, whereas the more compliant design (2B3) revealed inward motion at its edges. Alternatively, the circumferential stress values were dependent on both stent design and plaque material properties. Higher stresses were observed with the stiffer plaque, while comparison between designs showed the stiffer stent inducing higher stress values than the more compliant design across all plaque material properties. The smallest difference between stent designs occurred with the least stiff plaque. Furthermore, abrupt changes in stress values were observed at the stent edges, with larger changes seen with the stiffer stent.

It is thought that regions of high artery stress are the most susceptible to an adverse biological response. Thus, any chance to minimize such stresses while still maintaining arterial patency should be strongly considered. In the case of rigid, calcium-rich atherosclerotic plaques, the more compliant stent design (i.e., large strut spacing, radius of curvature, and axial amplitude) would be preferable to reduce unnecessary chronic trauma to the artery wall and still provide adequate radial rigidity to restore blood flow. When confronted with softer, lipid-laden plaques, a more rigid stent design (i.e., small strut spacing, radius of curvature, and axial amplitude) could be implanted, since either design induces a similar stress field. Such ''general'' design guidelines can be applied to interventional procedures with commercially available designs. Further advancements in imaging modalities and a more thorough investigation of the mechanical properties of diseased tissue will assist in designing stents for individual patients (i.e., lesion-specific stenting).

REFERENCES

1. Edelman ER, Rogers C. Pathobiologic responses to stenting. *Am J Cardiol*. 1998;81: 4E–6E.
2. Kastrati A, Mehilli J, Dirschinger J, et al. Restenosis after coronary placement of various stent types. *Am J Cardiol*. 2001;87:34–39.
3. Serruys PW, Kutryk MJ, Ong AT. Coronary-artery stents. *N Engl J Med*. 2006;354:483–495.
4. Joner M, Finn AV, Farb A, et al. Pathology of drug-eluting stents in humans: delayed healing and late thrombotic risk. *J Am Coll Cardiol*. 2006;48:193–202.
5. Duda SH, Bosiers M, Lammer J, et al. Drug-eluting and bare nitinol stents for the treatment of atherosclerotic lesions in the superficial femoral artery: long-term results from the SIROCCO trial. *J Endovasc Ther*. 2006;13: 701–710.
6. Holzapfel GA, Stadler M, Gasser TC. Changes in the mechanical environment of stenotic arteries during interaction with stents: computational assessment of parametric stent designs. *J Biomech Eng*. 2005;127:166–180.
7. Kiousis DE, Gasser TC, Holzapfel GA. A numerical model to study the interaction of vascular stents with human atherosclerotic lesions. *Ann Biomed Eng*. 2007;35:1857–1869.
8. Pulido MA, Angiolillo DJ, Costa MA. Imaging of atherosclerotic plaque. *Int J Cardiovasc Imaging*. 2004;20:553–559.
9. Lally C, Dolan F, Prendergast PJ. Cardiovascular stent design and vessel stresses: a finite element analysis. *J Biomech*. 2005;38: 1574–1581.
10. Bedoya J, Meyer CA, Timmins LH, et al. Effects of stent design parameters on normal artery wall mechanics. *J Biomech Eng*. 2006;128: 757–765.

11. Holzapfel GA, Sommer G, Regitnig P. Anisotropic mechanical properties of tissue components in human atherosclerotic plaques. *J Biomech Eng*. 2004;126:657–665.
12. Salunke NV, Topoleski LD, Humphrey JD, et al. Compressive stress-relaxation of human atherosclerotic plaque. *J Biomed Mater Res*. 2001;55:236–241.
13. Hayashi K. Experimental approaches on measuring the mechanical properties and constitutive laws of arterial walls. *J Biomech Eng*. 1993;115:481–488.
14. Higashida RT, Meyers PM, Phatouros CC, et al. Reporting standards for carotid artery angioplasty and stent placement. *Stroke*. 2004;35: e112–134.
15. Lyon RT, Zarins CK, Lu CT, et al. Vessel, plaque, and lumen morphology after transluminal balloon angioplasty. Quantitative study in distended human arteries. *Arteriosclerosis*. 1987;7:306–314.
16. Timmins LH, Moreno MR, Meyer CA, et al. Stented artery biomechanics and device design optimization. *Med Biol Eng Comput*. 2007;45:505–513.
17. Migliavacca F, Petrini L, Massarotti P, et al. Stainless and shape memory alloy coronary stents: a computational study on the interaction with the vascular wall. *Biomech Model Mechanobiol*. 2004;2:205–217.
18. Matsumoto T, Hayashi K. Stress and strain distribution in hypertensive and normotensive rat aorta considering residual strain. *J Biomech Eng*. 1996;118:62–73.
19. Smith JD, Davies N, Willis AI, et al. Cyclic stretch induces the expression of vascular endothelial growth factor in vascular smooth muscle cells. *Endothelium*. 2001;8:41–48.
20. Farb A, Weber DK, Kolodgie FD, et al. Morphological predictors of restenosis after coronary stenting in humans. *Circulation*. 2002;105:2974–2980.
21. Indolfi C, Torella D, Coppola C, et al. Rat carotid artery dilation by PTCA balloon catheter induces neointima formation in presence of IEL rupture. *Am J Physiol Heart Circ Physiol*. 2002;283:H760–767.
22. Colombo A, Hall P, Nakamura S, et al. Intracoronary stenting without anticoagulation accomplished with intravascular ultrasound guidance. *Circulation*. 1995;91:1676–1688.
23. Berry JL, Manoach E, Mekkaoui C, et al. Hemodynamics and wall mechanics of a compliance matching stent: in vitro and in vivo analysis. *J Vasc Interv Radiol*. 2002;13: 97–105.
24. Murray A, Allen V, Bennett MK. Validation of an automated technique for determining the mechanical characteristics of coronary arteries during balloon angioplasty: laboratory assessment with necropsy segments. *Heart*. 1998;79: 608–612.
25. Gasser TC, Holzapfel GA. Modeling plaque fissuring and dissection during balloon angioplasty intervention. *Ann Biomed Eng*. 2007;35: 711–723.
26. LaDisa JF, Olson LE, Molthen RC, et al. Alterations in wall shear stress predict sites of neointimal hyperplasia after stent implantation in rabbit iliac arteries. *Am J Physiol Heart Circ Physiol*. 2005;288:H2465–2475.
27. He Y, Duraiswamy N, Frank AO, et al. Blood flow in stented arteries: a parametric comparison of strut design patterns in three dimensions. *J Biomech Eng*. 2005;127:637–647.
28. Berry JL, Santamarina A, Moore JE, et al. Experimental and computational flow evaluation of coronary stents. *Ann Biomed Eng*. 2000;28:386–398.
29. Duraiswamy N, Schoephoerster RT, Moreno MR, et al. Stented artery flow patterns and their effects on the artery wall. *Annu Rev of Fluid Mech*. 2007;39:357–382.